Proceedings of the 17th World Congress
The International Federation of Automatic Control
Seoul, Korea, July 6-11, 2008

Motion Planning for Non-Holonomic Mobile Manipulator Based Visual Servo under Large Platform Movement Errors at Low Velocity

Le Minh Phuoc*,. Philippe Martinet**. Hunmo Kim*.Sukhan Lee****

**School of Mechanical Engineering, Sungkyunkwan University, Suwon Korea (e-mail: leminhphuoc@gmail.com, kimhm@me.skku.ac.kr).*
***Intelligent System Research Center, Sungkyunkwan University, Suwon Korea, (e-mail: Philippe.Martinet@lasmea.univ-bpclermont.fr, lsh@ece.skku.ac.kr)*

Abstract: A non-holonomic mobile manipulator (NMM) is termed here as a robotic system in which a manipulator is mounted on a non-holonomic mobile platform. This paper presents a method for planning a motion of NMM for effectively performing eye-on-hand visual servo especially when there are excessive errors in platform movement at low velocity due to friction, slippage, backlash, or flexibility. Due to excessive errors in platform movement at low velocity, direct application of a conventional method for manipulator based visual servo to an NMM may not be effective for generating servo motions. In this paper, we propose a method of generating servo motions for an NMM based visual servo, which is not affected by the excessive platform movement errors at low velocity. We achieve this by generating a series of discrete optimal poses of NMM on-line as a higher level plan for servo motion. More specifically, NMM is to move successively to the chosen poses while maintaining a proper velocity for avoiding excessive movement errors and satisfying non-holonomic constraints until it reaches the final poses where the manipulator alone can servo to the target object while the platform can be kept stationary. We use the virtual visual servo by E. Marchand and F. Chaumette to make sure that the manipulator is able to reach a target object without violating its joint limits, its boundary of workspace and singularities. The on-line selection of local mobile platform poses is based on a local random search. Finally, simulations on a redundant NMM are carried out to demonstrate the effectiveness of the proposed method.

1. INTRODUCTION

Mobile manipulators have become very popular in robotics research as well as in applications such as manufacturing environment, home environment and space robotics. The reason for using such robotic systems is that the manipulator can cover a larger workspace thanks to high mobility from mobile platform. A mobile manipulator subject to non-holonomic constraint in the mobile platform is known as a non-holonomic mobile manipulator (NMM).

One of the most challenging issues in NMMs research is to ensure precise control of the whole system. In order to solve the problem, the issue of coordination between mobile platform and manipulator was developed (Carriker *et al.*, 1991), (H. Seraji, 1993). Moreover, it is well known that visual servoing scheme was proposed for robot control in order to increase the robustness to uncertainties as well as achieve higher accuracy in positioning (S. Hutchinson *et al.*, 1996). Therefore, visual servoing was implemented on NMMs in recent years (A. D. Luca *et al.*, 2006), (D. Tsakiris *et al.*, 1998). On a real robotic system, there are many other aspects, which seriously affect the accuracy of robot control, such as tip vibration (Q. Huang and S. Sugano, 1996), dynamical effects (Y. Yamamoto and X. Yun, 1997). In order to guarantee precise manipulation on a mobile platform with only kinematics, we share the idea with (S. Dong Hun *et al.*, 2003) by commanding mobile platform to move in discrete steps. However, it is noted that our approach still preserves the full body motion of NMM when the platform operates at high velocities. At low velocities of mobile platform, the dynamic effects from the system such as friction and backlash seriously reduce the precision of the mobile platform and consequently the whole system. Hence, the platform has to move in discrete steps and continuously reposition itself whenever the manipulator is approaching joint limits and singularities. Moreover, in (S. Dong Hun *et al.*, 2003), mobile platform is placed based on manipulability (T. Yoshikawa, 1985), which is an index dependent only on the current configuration of system. Our proposal is based on another index which is dependent not only on the configuration but also how good the performance of the manipulator achieving the task by virtual visual servo technique (E. Marchand and F. Chaumette, 2002).

The paper is set out as follows: firstly, the kinematic modelling of NMMs is presented, together with an overview of visual servo control scheme. Then, the motivations of the work, proposed method as well as algorithm are developed in detail. Finally, a simulation of the new method on a ten degree of freedom NMM is presented to demonstrate the concepts and likely benefits.

2. FUNDAMENTALS

2.1 Kinematics modelling of NMMs

For the purpose of visual servoing, the differential kinematics of NMMs need to be considered. Assume that $Z \in \mathbb{R}^r$ is the

kinematic function of the whole NMM system. The kinematic function is chosen based on tasks to be performed by the system. The kinematic function is described as follow with respect to the system configuration vector $q = [q_p \quad q_m]^T$, where $q_p \in \mathbb{R}^{n_p}$ and $q_m \in \mathbb{R}^{n_m}$ respectively, are the generalized coordinates of the platform and the manipulator.

$$Z = f(q_p, q_m) \tag{1}$$

Since the platform is subjected to non-holonomic constraint, the kinematic model of the platform can be rewritten with respect to its controllable velocity inputs $u_p \in \mathbb{R}^{c_p}$ with $c_p < n_p$ and the non-holonomic constraint matrix G .

$$\dot{q}_p = G(q_p)u_p \tag{2}$$

Following the kinematic model formulation of general NMMs by De Luca *et al.* (De Luca, Oriolo *et al.* 2006), the differential kinematic model of the whole system is given as follows:

$$\begin{aligned} \dot{Z} &= J_p(q)G(q_p)u_p + J_m(q)u_m \\ &= \begin{bmatrix} J_p(q)G(q_p) & J_m(q) \end{bmatrix} \begin{bmatrix} u_p \\ u_m \end{bmatrix} = J(q)u \end{aligned} \tag{3}$$

where J is the Jacobian of NMM and, $u_m \in \mathbb{R}^{c_m}$ are the velocity input of the manipulator.

2.2 Eye-on-hand position based visual servoing control

Several visual servoing control schemes have been proposed in literatures such as position based, image based and hybrid based control (S. Hutchinson *et al.*, 1996). It is claimed that position based visual servo is sensitive to model error and camera calibration error (F. Chaumette, 1998). However, position based visual servo does not encounter potential image local minima as well as image singularities (F. Chaumette, 1998). In the proposed scheme, due to high mobility of the system and consequently the need to follow a long visual servo trajectory, position based visual servo scheme with eye-on-hand configuration (B. Thuilot *et al.*, 2002) has been adopted. The frame assignment is shown in fig. 1.

Assume that s denotes the visual features of the visual servoing scheme

$$s = \begin{pmatrix} t \\ u\theta \end{pmatrix} \tag{4}$$

where t is the translational part of the homogeneous matrix ${}^{\mathcal{T}}T_{\mathcal{G}}$, and $u\theta$ is the axis/angle representation of the rotational part of ${}^{\mathcal{T}}T_{\mathcal{G}}$ .The matrix ${}^{\mathcal{T}}T_{\mathcal{G}}$ shows relation between robot's hand and final target pose. It is computed from observation of object from an embedded camera on robot hand as following.

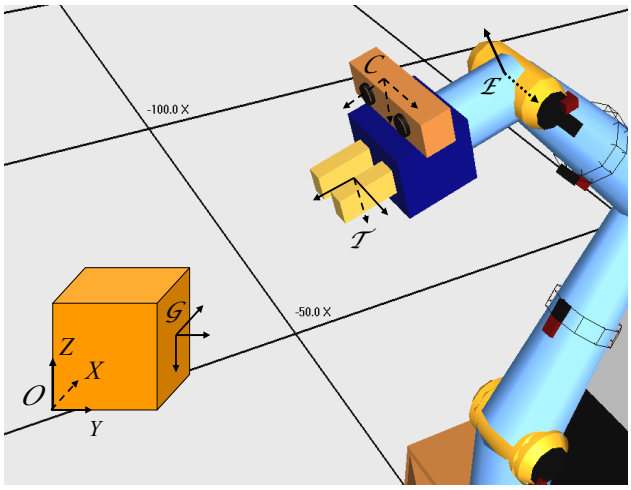

Fig. 1. Frame assignment in eye-on-hand position based visual servoing scheme

$${}^{\mathcal{T}}T_{\mathcal{G}} = \left({}^{\mathcal{F}}T_{\mathcal{T}}\right)^{-1}.{}^{\mathcal{F}}T_{C}.{}^{C}T_{O\mathcal{P}}.\left({}^{O}T_{O\mathcal{P}}\right)^{-1}.{}^{O}T_{\mathcal{G}} \tag{5}$$

where ${}^{\mathcal{F}}T_{C}$ is the transformation between the robot's end effector and embedded camera on the robot's hand. ${}^{C}T_{O\mathcal{P}}$ is an estimation of an arbitrary object frame pose, expressed in camera frame. The pose estimation of object is computed by Lagrange-Lowe algorithm from an artificial maker attached on object. The pose position of artificial marker is known in object reference frame by the transformation ${}^{O}T_{O\mathcal{P}}$. Finally, the goal pose of the robot's hand with respect to the object's reference frame is determined in each application by ${}^{O}T_{\mathcal{G}}$.

Classical visual servoing gives the velocity in the gripper as,

$$\tau_{\mathcal{T}} = -\lambda e + \frac{\widehat{\partial e}}{\partial t} \tag{6}$$

where $e(s, s*) = \widehat{L_s^+}(s - s*)$. The last term $\frac{\widehat{\partial e}}{\partial t}$ is an estimation of visual feature changing over time. In other words, it is related to the motion of the object. In this case, the object is fixed and therefore, this term can be neglected. The interaction matrix $\widehat{L_s}$ can be set for the case of position based visual servoing (P. Martinet *et al.*, 1999) and hence, the input joint velocities sent to control robot are computed as follows:

$$\dot{q} = J^{-1} \begin{pmatrix} {}^{\mathcal{F}}R_{\mathcal{T}} & \left[{}^{\mathcal{F}}t_{\mathcal{T}}\right]_{\times}{}^{\mathcal{F}}R_{\mathcal{T}} \\ 0_{3\times 3} & {}^{\mathcal{F}}R_{\mathcal{T}} \end{pmatrix} .\tau_{\mathcal{T}} \tag{7}$$

where J is the robot Jacobian expressed in the robot end effector frame ,and ${}^{\mathcal{F}}R_{\mathcal{T}}$ and ${}^{\mathcal{F}}t_{\mathcal{T}}$ are, respectively, rotational part and translational part of the homogeneous transformation matrix ${}^{\mathcal{F}}T_{\mathcal{T}}$.

3. SEQUENCE OF OPTIMAL MOBILE PLAFORM POSES

3.1 Mobile platform motion at low velocities

In NMMs, it is common that the mobile platform encounters difficulties in achieving precise control. The wheels of the mobile platform face a nonlinear phenomenon, friction, due to the heavy weight of system. For example, the weight of only PowerBot from ActivMedia Robotics, which is used in this experiment, is approximately 140 kg. At low velocities of the mobile platform, this nonlinearity is more serious and it obstructs the desired motion or even creates slip-stick motion of the platform as shown in figure 2. Another nonlinearity occur at the platform is backlash. This also creates vibration of the whole robotic system whenever the platform reaches rotational velocity nearby zero and frequently changes its sign. The combination of the two nonlinear phenomena seriously impedes precise control of the platform at low velocities. In addition, precise control of the non-holonomic mobile robot is not possible at low velocities. Consequently, motion of the end-effector is not achievable in the final stages of visual servoing where the joint velocities of system approach zeros.

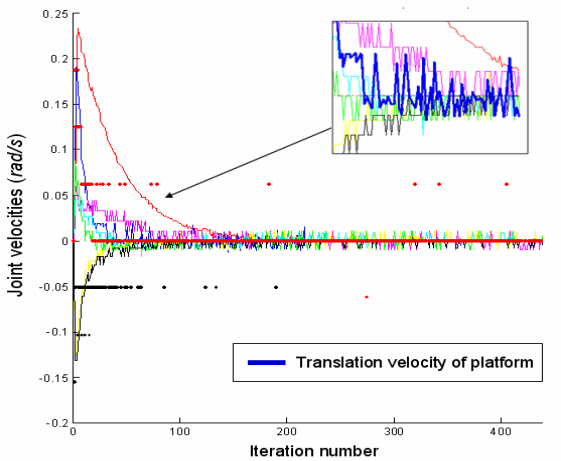

Fig. 2. Joint velocities during a classical mobile manipulator visual servoing. The fluctuation of translational velocity of the platform is shown at upper right picture.

3.2 Proposed method

Due to the difficulties in achieving precise control of the mobile platform at low velocities as discussed above, the mobile base is only commanded to move in discrete steps within the low range of mobile platform velocities (translational velocity and rotational velocity). As shown in fig. 3, the mobile manipulator visual servoing switches from full body motion in which the mobile base and manipulator operate continuously and simultaneously, FULLBODY_VS ; to discrete steps of the base in which the manipulator only servos a target object, ARM_VS, while the mobile platform is static. This happens when the mobile platform velocities reach a threshold ε_{p_1} or ε_{p_2}, corresponding to linear velocity and rotational velocity of platform, respectively. Values of these thresholds are currently selected in a heuristic way, depending on the mechanical properties of each system such as the weight of system, backlash of the power train, etc. Another indirect factor also contributing to the selection of the threshold is the performance of the mobile platform's low-level controller.

```
NMM_VISUAL_SERVOING
1   error ← Task;
2   while error < ε_e
3     if (u_p1 < ε_p1) or (u_p2 < ε_p2) then
4       if ARM_REACH_TARGET(error, J_m) then
5         ARM_VS (error, J_m);
6         if ARM_IN_CONSTRAINT(constraints) then
7           GET_OPTIMAL_BASEPOSE(best_BPose);
8           MOVE(best_BPose);
9       else
10        GET_OPTIMAL_BASEPOSE(best_BPose);
11        MOVE(best_BPose);
12    else
13      FULLBODY_VS (error, J);
14  return TRUE
```

Fig. 3. Algorithm of our proposed NMM visual servoing

It is obvious that the positions of the mobile platform strongly affect the performance of the visual servo as well as the completeness of the task. Thus, the mobile platform has to reposition itself whenever the manipulator is approaching its geometric constraints such as joint limits, singularities by checking ARM_IN_CONSTRAINT. Another case is that the system must compute an optimal pose of platform as that the manipulator realizes it cannot independently reach the target object by checking virtual visual servoing with ARM_REACH_TARGET. After the optimal pose of mobile platform is obtained with GET_OPTIMAL_BASEPOSE, the mobile platform will move to that pose by MOVE while the manipulator changes its configuration to satisfy the movement of the platform as well as keeping the target object in field of view of embedded camera. Details of these aspects are discussed later.

In order to get the optimal pose of the mobile platform as shown by the algorithm in fig. 4, a number of positions of mobile platform are randomly scattered around its current position by RAND_BPOSE. This function generates the mobile platform's pose that satisfies the non-holonomic constraint by forward integrating platform's kinematic function over a limited time with randomly generated controllable platform velocities (G. Oriolo and C. Mongillo, 2005). At each random mobile platform's pose, the manipulator has to be checked its reachability ARM_REACHABILITY from the new pose of platform to *Next_EEFPose*. If the new configuration of the entire system is validated, a virtual visual servoing VIRTUAL_VS is performed from the new configuration to the final target. At each random pose of the base, the performance of virtual

visual servo is measured by $VVS\_quality[a]$. After this step, a new loop to create a random pose of platform is performed. Finally, $VVS\_quality$ of all positions of platform are compared and returned to the optimal pose by COMPUTE_BEST_POSE.

GET_OPTIMAL_POSE
1 **for** $a = 1$ to NUM_RANDOM
2 $q_{p\_rand} \leftarrow$ RAND_BPOSE($q_p, u_{p_{1\max}}, u_{p_{2\max}}$);
3 $VVS\_quality[a] \leftarrow 0$;
4 GET_NEXT_EEFPOSE(*Next_EEFPose*);
5 **if** ARM_REACHABILITY(q_{p_rand}, *Next_EEFPose*)
6 **then**
7 $q_m \leftarrow$ ARM_INV_KINEMATICS(*Next_EEFPose*);
8 $q_{VVS} \leftarrow q +$ GET_NEW_JOINT(q_{p_rand}, q_m);
9 $VVS\_quality[a] \leftarrow$
10 VIRTUAL_VS(q_{VVS}, *Next_EEFPose, constraint*);
11 **return** COMPUTE_BEST_POSE($VVS\_quality$);

Fig. 4. Algorithm to get optimal pose of mobile platform

Since the new pose of platform is generated with random controllable velocities of platform and integrated over a limited time, the new pose of the mobile platform is locally optimal pose. However, it is noted that the platform continuously searches for the optimal poses whenever the manipulator reaches its geometric constraints. Hence, a series of optimal poses is formed in our method.

It is noted that the optimal pose of mobile platform is checked by comparing the performance of virtual visual servo. Thus, the optimal position of the mobile platform includes the meaning that the longer of the arm operate without changing base position, the better the mobile base position is.

Using this paradigm, the system changes its mobile platform pose and temporarily releases the main task. However, the embedded camera on the end-effector has to be controlled in order to keep visual features in the field of view. A simple constraint on end-effector's movement as shown in fig. 5 is utilized in our scheme. While the mobile platform is changing its pose, the end-effector has to reorient itself only in the plane parallel with the plane platform moving. Supposing that the manipulator does not change its configuration during platform's move, the error between end-effector and target object reduces from r_1 to r_2, and the angle α can be found based on the movement of the platform. Then the end-effector reorients itself based on both angle α and the changing pose of the platform. At each random mobile platform pose, the manipulator has to be checked its reachability from the new pose of platform to the new end-effector pose. If the manipulator has closed-form inverse kinematics solution, the reachability can be checked very fast. In the case of that the manipulator is a redundant one, there may be more than one solution of inverse kinematics. The selection of the best solution is another issue,

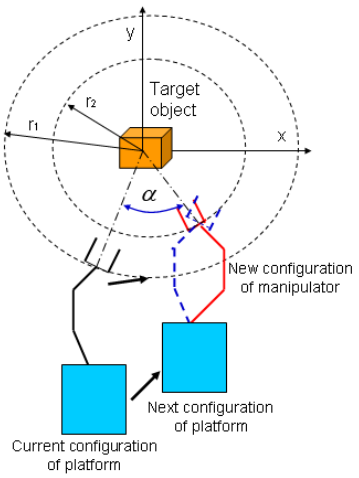

Fig. 5. The method to keep visual features in embedded camera's field of view while the platform moves between discrete steps

depending on redundancy analysis of the manipulator. Currently, an arbitrary solution is chosen for the next step in order to preserve the randomized property of the approach.

The performance of visual servoing in this case depends on the completeness to visual servo task, convergence speed of visual servo and geometric constraints that the system encounters during visual servo. The virtual visual servo technique is an effective way to evaluate the visual servo performance of the system. However, it has draw back due to the trade off between computation time and the completeness in running virtual visual servo.

4. IMPLEMENTATIONS

The proposed method is simulated on an NMM with seven degree of freedom manipulator as shown in fig. 6. The manipulator has structure similar to a human arm in which joints are successively perpendicular. This manipulator has a closed-form inverse kinematic solution (P. Dahm and F. Joublin, 1997) and the reachability of this manipulator is implemented based on this solution. In this simulation, the two criteria used for switching from full mobile manipulator visual servoing phase to mobile manipulator with discrete movement of mobile platform are joint limits and

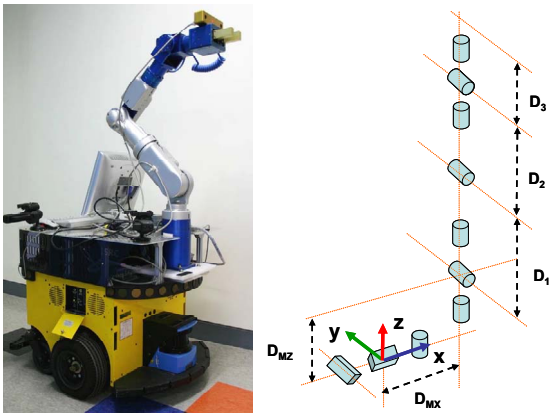

Fig. 6. A NMM and its kinematic structure used to simulate our approach

singularities. The joint limits here are not hard joint limits of from the specification of the system but soft joint limits (E. Marchand *et al.,* 1996), which allow for a region of safety with respect to the real limits. Singularities of the manipulator are detected by monitoring smallest singular value of the manipulator's Jacobian matrix (A.A. Maciejewski *et al*., 1988).

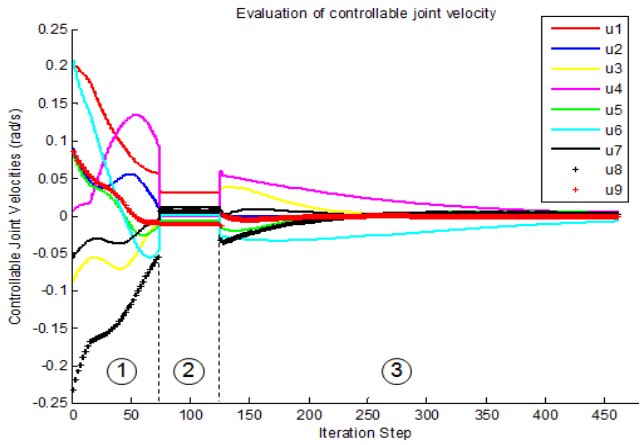

Fig. 7. Joint velocity during visual servoing. Region 1,2 and 3 correspond to mobile manipulator visual servo phase, moving to optimal pose phase and only manipulator visual servo phase, respectively

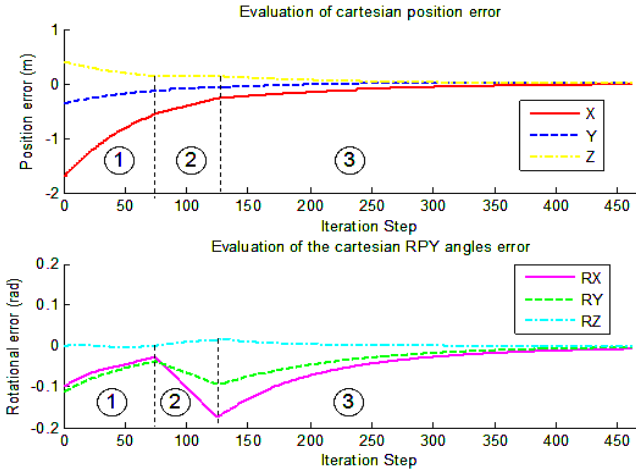

Fig. 8. Cartesian error during visual servoing. Region 1,2 and 3 correspond to mobile manipulator visual servo phase, moving to optimal pose phase and only manipulator visual servo phase, respectively

Moreover, the performance of virtual visual servoing or quality of virtual visual servoing in fig. 3 is calculated based on how fast the virtual visual servo converges to the final target and whether the process violates joint limits and singularities. By comparing virtual visual servoing, the optimal pose of the platform could be found. Virtual visual servoing quality is calculated as follows.

$$VVS\_quality = \begin{cases} 0 & if\ arm\ reach\ joint\ limits / singularites \\ VVS\_iteration & otherwise \end{cases} \quad (11)$$

Another issue which has to be noted during implementation of this method is the changing configuration by robot's internal motion. Because the new configuration of the system basically originates from probabilistic approach, the new configuration might not be reached from the current configuration. The reason is that the internal motion of robot is based on Jacobian and the motion could meet local minima.

Table 1. Related parameters and runtimes

Quantity	Values
Number of random platform configurations	50
Limited time in a reachable set	1.5
Min/Max random linear velocity	-0.2/0.2 m/s
Min/Max random rotational velocity	-0.2/0.2 rad/s
Number of platform configuration is reachable by manipulator	37
Time for virtual visual servoing	7.8 s
Average time for checking reachability	5.73 ms

The proposed method is tested with the parameters given in table 1 and the minimum of translational platform velocity and rotational platform velocity are set at 0.015 m/s and 0.015 rad/s respectively. The system should switch to only manipulator visual servo at those thresholds.

The proposed visual servoing scheme includes three phases of motion. In the first phase, a full body visual servoing is performed. In the second phase, the system changes configuration to the optimal configuration while keeping visual features of the target in camera view. In the last phase, only the manipulator does visual servo to the target. The velocities of all joints are shown in fig. 7. Cartesian error between the end-effector and the target object during the proposed scheme is displayed in fig. 8. It is shown that Cartesian errors in both positions and angles converge to

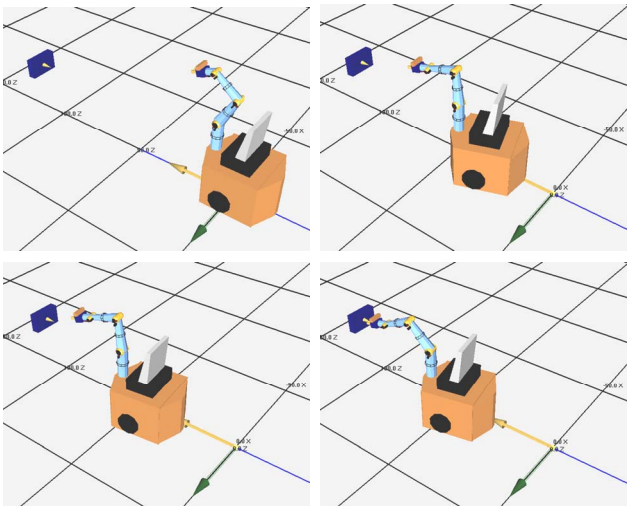

Fig. 9. Motion of system during visual servoing

zeros finally. The change of system configuration to the optimal pose of the platform leads to temporary divergence of angle error in the second phase of motion. This motion keeps target objects in the embedded camera's field of view. Finally, motion of the whole system is captured in fig. 9.

5. CONCLUSIONS AND DISCUSSION

This This paper has presented a scheme of NMM visual servo with the imprecision movement of the mobile platform at low velocities of platform. It has been shown that the visual servo task on NMMs can be achieved with discrete steps of the mobile platform at the last minute of visual servoing. At high velocities of mobile platform, full NMM visual servoing is still preserved. The mobile platform is placed at optimal poses by comparing virtual visual servoing performance to the final target with respect to joint limits and singularities. The optimum in this case implies that the platform is placed so that the manipulator has optimal performance of the task but not the optimal configuration at that moment. Although there is not a series of optimal poses of platform in the experimental result, it does show that the algorithm can generate an optimal pose for the platform to reach the final target without violating manipulator joint limits or singularities.

However, there are also some issues are raised from the scheme. The sampling region is currently determined by heuristic approach. The size of this region leads to the problem of global optimum and local optimum in selection of mobile pose. Ensuring smoothness in the transition from one phase of motion to another is also important aspect of the research that will be undertaken in the future work.

ACKNOWLEGEMENT

This work is supported by Intelligent Robotics Program, one of the 21st century Frontier R&D Program funded by the Ministry of Commerce, Industry, and Energy of Korea. This work is also supported in part by the Korea Research Foundation.

REFERENCES

A. A. Maciejewski and C.A. Klein, "Numerical filtering for the Operation of robotic manipulators through kinematically singular configurations", *Journal of Robotic Systems,* **vol. 5**, pp. 527-552, 1988.

A. D. Luca, G. Oriolo, and P. R. Giordano, "Image-based visual servoing schemes for nonholonomic mobile manipulators " *Robotica,* **vol. 25**, pp. 131-145, 2007.

A. De Luca, G. Oriolo, and P. R. Giordano, "Kinematic modeling and redundancy resolution for nonholonomic mobile manipulators," in *IEEE International Conference on Robotics and Automation*, 2006, pp. 1867-1873.

B. Thuilot, P. Martinet, L. Cordesses, and J. Gallice, "Position based visual servoing: keeping the object in the field of vision", *in Proceedings of theIEEE International Conference on Robotics and Automation*, *ICRA'02*, pp.1624-1629, Washington DC, USA, May, 2002

D. Tsakiris, P. Rives, and C. Samson, "Extending Visual Servoing Techniques to Nonholonomic Mobile Robots," in *Lecture Notes in Control and Information Systems (LNCIS)*, G. Hager, D. Kriegman, and S. Morse, Eds.: Springer-Verlag, 1998.

E. Marchand and F. Chaumette, "Virtual Visual Servoing: a framework for real-time augmented reality," in *EUROGRAPHICS'02*, 2002, pp. 289-298.

E. Marchand, A. Rizzo, and F. Chaumette, "Avoiding robot joint limits and kinematics singularities in visual servoing," in *Proc. 13th Int. Conf. Pattern Recognition, ICPR'96*, Vienna, Austria, 1996, pp. 297-301.

F. Chaumette, "Potential problems of stability and convergence in image-based and position-based visual servoing" in *The Confluence of Vision and Control*. **vol. 237**: Springer-Verlag, 1998, pp. 66-78.

G. Oriolo, C. Mongillo, "Motion Planning for Moible Manipulators along Given End-effector Paths", in *IEEE International Conference on Robotics and Automation*, 2005, pp. 2154-2160, Bacerlona, Spain, April 2005.

H. Seraji, "An on-line approach to coordinated mobility and manipulation," in *IEEE International Conference on Robotics and Automation*, 1993, pp. 28-35 **vol.1**.

P. Dahm and F. Joublin, "Closed form solution for the inverse kinematics of a redundant robot arm," Institute for Neuroinformatic Lehrstuhl fur Theoretische Biologie, Ruhr-University, Bochum, Germany.

P. Martinet, J. Gallice, "Position based visual servoing using a nonlinear approach", *in Proceedings of the IEEE/RSJ International Conference on Intelligent Robots and Systems, IROS'99*, **vol. 1**, pp. 531-536, Kyongju, Korea, October 17-21th, 1999

Q. Huang and S. Sugano, "Motion planning of stabilization and cooperation of a mobile manipulator-vehicle motion planning of a mobile manipulator," in *IEEE/RSJ International Conference on Intelligent Robots and Systems '96, IROS 96,* , 1996, pp. 568-575 **vol.2**.

S. Dong Hun, B. S. Hamner, S. Singh, and H. Myung, "Motion planning for a mobile manipulator with imprecise locomotion," in *IEEE/RSJ International Conference on Intelligent Robots and Systems, 2003. (IROS 2003).* , 2003, pp. 847-853 **vol.1**.

S. Hutchinson, G. D. Hager, and P. I. Corke, "A tutorial on visual servo control," *Robotics and Automation, IEEE Transactions on,* **vol. 12**, pp. 651-670, 1996.

T. Yoshikawa, "Manipulability of robotic mechanism," *International Journal of Robotics Research,* **vol. 2**, pp. 113-124, 1985.

W. Carriker, P. Khosla, and B. Krogh, "Path planning for mobile manipulators for multiple task execution," *IEEE Transaction on Robotics and Automation,* **vol. 7**, pp. 403-408, 1991.

Y. Yamamoto and X. Yun, "A modular approach to dynamic modeling of a class of mobile manipulators," *International Journal of Robotics and Automation,* **vol. 12**, pp. 41-48, 1997.

Y. Yamamoto and X. Yun, "Coordinating locomotion and manipulation of a mobile manipualtor," *IEEE Transaction on Automatic Control,* **vol. 39**, pp. 1326-1332, 1994.